Thin-Walled Structures 49 (2011) 85–93

Contents lists available at ScienceDirect

Thin-Walled Structures

journal homepage: www.elsevier.com/locate/tws

Prediction of the squash loads of concrete-filled tubular section columns with local buckling

Young Bong Kwon [a,*], Sang Jung Seo [a], Doo Won Kang [b]

[a] Department of Civil Engineering, Yeungnam University, Gyongsan 712-749, Republic of Korea
[b] Department of Civil Engineering, Lotte Construction and Consulting Co. Ltd., Seoul 137-723, Republic of Korea

ARTICLE INFO

Article history:
Received 1 February 2010
Accepted 23 August 2010
Available online 15 September 2010

Keywords:
Circular hollow steel (CHS) sections
Concrete-filled tubular (CFT) sections
Squash load
Ultimate strength
Compression tests
Diameter to thickness ratio
Width to thickness ratio
Direct strength method

ABSTRACT

This paper describes a series of compression tests of circular hollow steel (CHS) sections and circular concrete-filled tubular (CFT) sections. The diameter to thickness ratios of the test specimens ranged 45–140. This range was set to investigate the effect of local buckling in the circular steel skin on the ultimate strength of CFT columns. The confining effect against filled-in concrete was also studied. A squash load formula for CFT stub columns is proposed to account for the post-local-buckling strength of steel skin. The ultimate strength of steel skin was predicted by a kind of Direct Strength Method (DSM). The proposed DSM does not require the computation of the effective area of the steel skin, but uses the gross area of the steel skin and the design strength formula based on various test results. The compressive strength formula of the filled-in concrete accounting for the strength ratio of steel skin to filled-in concrete is also proposed to consider the increase in compressive strength of the filled-in concrete, due to the confining effect of the steel skin. The design strengths of CFT columns were compared with the test results for verification.

1. Introduction

The attractive way to solve the local instability and the low ductility of thin hollow steel tubes is filling them with concrete. The concrete-filled tubular (CFT) composite sections are being widely used as columns of high-rise buildings and bridge piers in recent years. Since the steel skin confines the filled-in concrete tri-axially and the concrete resists against the inward deformation of steel skin, both steel and concrete contribute to the strength enhancement of the CFT column.

The CFT columns are susceptible to local buckling of the steel skin, which in many cases is very thin. The post-local-buckling strength of the steel skin and the concrete compressive strength due to tri-axial confinement by the locally buckled steel skin, both of which contribute to the ultimate strength of CFT columns, need to be estimated accurately to predict the ultimate strength of CFT columns reasonably. The confining effect of a steel skin can increase the concrete compressive strength beyond $0.85F_c$. However, since micro-cracking can reduce the tri-axial effect, Chen and Atusta [1] and Bradford [2] have conservatively suggested that the effective strength of concrete in a steel casing should not exceed $0.85F_c$. The Eurocode4 (2004) [3] has the provision, where $1.0F_c$ can replace $0.85F_c$ for the concrete-filled hollow sections and some additional amount of strengths can be considered for circular composite tubes, and the AISC specifications (2005) [4] applies $0.85F_c$ as the limit for rectangular concrete-filled tubular steel sections and $0.95F_c$ for circular concrete-filled tubular steel sections.

In this paper, a series of compression tests of circular hollow steel (CHS) sections and circular concrete-filled tubular sections were conducted. Since the steel tubes for CFT columns are usually thin, they may be subjected to the effects of local buckling. Local buckling of the steel skin occurs before the critical stress of the steel skin reaches the yield stress; in such a case, post-local-buckling can affect the ultimate strength of the composite sections. The diameter-thickness ratio of the test specimens ranged 45–140; this range was selected to study the correlation between the compressive strength of the filled-in concrete and the local buckling stress of the circular steel skin. Simple ultimate strength formulae for the steel skin were developed to account for the local buckling stress and the post-local-buckling strength reserve. While the post-local-buckling strength reserve may be included in the current design specifications such as AASHTO specifications (2007) [5], AISC specifications (2005) [4], Eurocode4 (2004) [3] by the Effective Width Method, the strength formula for the Direct Strength Method [6,7] proposed does not need to compute the effective area of the steel skin, and uses the gross area of the steel skin. The strength formula uses the elastic local buckling stress of the steel skin, which can be computed by a rigorous analysis program or theoretical equations, and the ultimate strength formula based on the various test results. A design compressive strength formula for the filled-in concrete is also proposed to account for the strength ratio of the steel skin and filled-in concrete and the local buckling stress of the steel skin. The formula proposed can consequently account for the increase in compressive strength of

* Corresponding author. Tel.: +82 11 802 2418; fax: +82 53 810 4622.
E-mail address: ybkwon@ynu.ac.kr (Y. Bong Kwon).

0263-8231/$ - see front matter © 2010 Elsevier Ltd. All rights reserved.
doi:10.1016/j.tws.2010.08.009

the filled-in concrete, due to the confining effect of the steel skin against the outward deformation of filled-in concrete. The design strengths of circular and rectangular CFT columns predicted by the proposed strength formulae were compared with the current specifications and previous test results.

2. Material and section properties

The tensile coupon test was performed to determine the mechanical properties of the test sections. The tensile coupon test results showed that the yield and the ultimate stresses were higher than the nominal strengths. The average values of stresses and strains are summarized in Table 1. The average yield stress is higher than the nominal yield stress by approximately 10.4% and the average ultimate tensile stress is higher than the nominal tensile stress by 18.5%. To determine the compressive strength of the filled-in concrete, 6 cylinders (10 cm in diameter × 20 cm in height) were cast from the same batch concrete used as filled-in concrete for concrete-filled composite sections. The measured average compressive strength and Young's Modulus of concrete were 25.4 and 23,690 MPa, respectively.

A series of compression tests were performed on the circular hollow steel (CHS) sections and circular concrete-filled tubular (CFT) sections to investigate the structural behavior and performance of CFT columns. The thickness of the test sections was 3.2 mm, and the nominal yield and ultimate stresses were 240.0 and 400.0 MPa, respectively. The test sections shown in Fig. 1 were fabricated by continuous gas welding. End plates of 30 mm in thickness were welded to both ends of the specimens to minimize eccentric loading and to prevent local failure of the specimen ends. A 100.0 mm hole for concrete casting was pre-cut in the bottom end plate. The detailed dimensions of the test columns are listed in Table 2. The diameter to thickness ratios of the test sections ranged 47.2–140.6, which was selected to be somewhat lower or higher than the yield limit ratio of 90–100 provided in the current specifications, such as AISC (2005) [4] and EC4 (2004) [3]. The column lengths were three or four times the diameter of the test sections, and the slenderness ratios (L/r) were approximately between 9.0 and 12.0. Therefore, since overall buckling was not likely to occur, local buckling and post-local-buckling strength or yielding of the sections was expected to govern the member strength of the test columns. For the sections of large diameter to thickness ratios, local buckling of the steel skin was expected to occur before the first yield of the material. The post-buckling strength in a local mode should be accounted to accurately predict the ultimate strength of CFT columns.

Table 1
Material properties of steel.

Steel	F_y(MPa)	F_u(MPa)	ε_y	ε_u	E_s(MPa)
	265.0	474.0	0.0016	0.241	205,700

3. Column tests

3.1. CHS column tests

A series of compression tests were performed to investigate the buckling and the ultimate strengths of CHS columns. The loaded end was hinged and the bottom end was fixed. A concentric compression test was conducted, using a 3000 kN

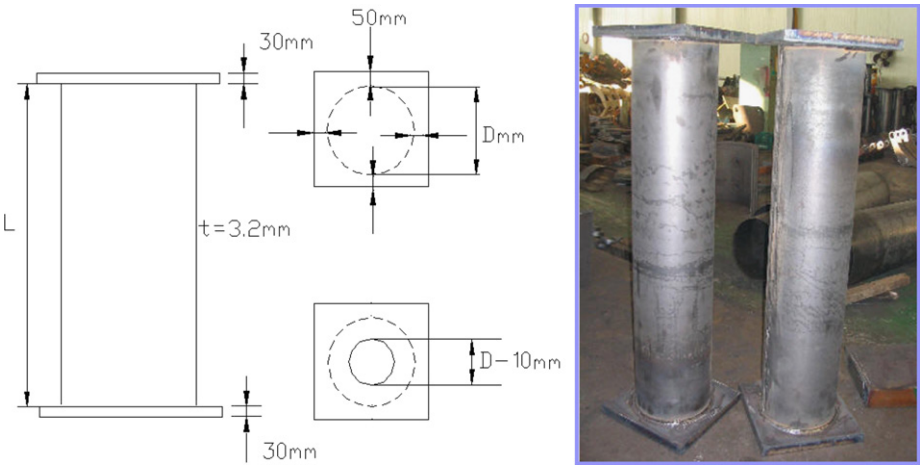

Fig. 1. Test sections.

Table 2
Geometries of CHS and CFT sections.

Specimens	D(mm)	t(mm)	D/t	L/r	L(mm)	As(mm^2)	Ac(mm^2)	nAs+Ac(mm^2)
SC-47	151.0	3.2	47.2	11.9	620	1486	16,422	29,796
SC-47a	150.0	3.2	47.1	11.9	620	1476	16,196	29,480
SC-62	199.0	3.2	62.2	12.1	835	1968	29,134	46,819
SC-62a	198.0	3.2	61.9	12.1	835	1958	28,832	46,454
SC-78	251.0	3.2	78.4	12.0	1050	2489	46,990	69,391
SC-94	300.0	3.2	93.8	11.9	1250	2989	67,702	94,603
SC-109	350.0	3.2	109.4	12.0	1468	3487	92,725	124,108
SC-125	401.0	3.2	125.3	11.9	1680	4000	122,294	158,294
SC-140	450.0	3.2	140.6	12.0	1888	4493	154,551	194,988

Shimazu Universal Testing Machine. Downward loading was controlled by the displacement control method at the loading velocity of 0.01 mm/s. Vertical displacement was obtained from the machine directly and horizontal displacements were measured by displacement transducers, which were attached at the center and at the quarter points of the test specimens. Since the local buckling stress was slightly lower than the yield stress, elastic local buckling did not occur even for the section with D/t ratio larger than 100 during testing. Inelastic local buckling occurred with different numbers of lobes along the columns and buckle waves in the circumference. Deformation due to local buckling increased according to the increase of load, until the maximum load was reached. The typical final collapse mode of the CHS section is shown in Fig. 2. Most sections showed kinks across the section. However, some of the sections finally collapsed because the half-wave, which was located near the bottom end of the columns, was flattened out into a rhombus or triangle shape shown in Fig. 2. Although both the number of buckle half-waves in the cross section and the number of lobes along the column were different between test sections, the final collapse modes were quite similar except at the locations of the kinks.

The axial load-shortening curves of the CHS columns tested are shown in Fig. 3. As shown in the figure, as the compressive load was increased after the initial take-up of loading, most specimens showed a linear load versus shortening behavior before the occurrence of local buckling at several locations along the column. After the maximum load, the column of low D/t ratio did not collapse abruptly, but showed a stable behavior. However, in the case of the sections of large D/t ratio, the column displayed a fairly sharp drop of axial load in comparison with the columns of low D/t ratio. The sections of high D/t ratios showed a significant post-local-buckling strength reserve up to the ultimate load. However, after the peak load was reached, the load decreased more sharply than the sections of low D/t ratios.

The test ultimate and the local buckling stresses of the CHS sections are compared with the inelastic analysis results obtained, using the LUSAS (ver. 14.3) [8] in Table 3. In the FE analysis, an elastic buckling analysis was conducted first and the local buckling mode was assumed as the initial imperfections, where the magnitude was taken as $t/100$. An elastic-perfect plastic stress–strain relation was assumed and the von-Mises yield criteria were applied. The local buckling stresses, f_{crl}, for the sections of D/t ratios 47 and 62 were higher than the nominal yield stress of 240.0 MPa. The local buckling stresses of the sections whose D/t ratios were higher than 78 were estimated to be lower than the nominal yield stress. However, regardless of the D/t ratios, the maximum stresses, f_{max}, of all the test sections were higher than the test yield stress of 265.0 MPa, due to a significant post-local-buckling strength reserve. The higher the diameter-thickness ratio was, the larger the post-local-buckling strength reserve was. The elastic local buckling stresses of the test sections were much higher than the test yield stress, which meant that most of the test sections underwent inelastic local buckling and some of them yielded to failure. The maximum D/t limit of 90–100 for the yield criteria in current specifications such as AISC

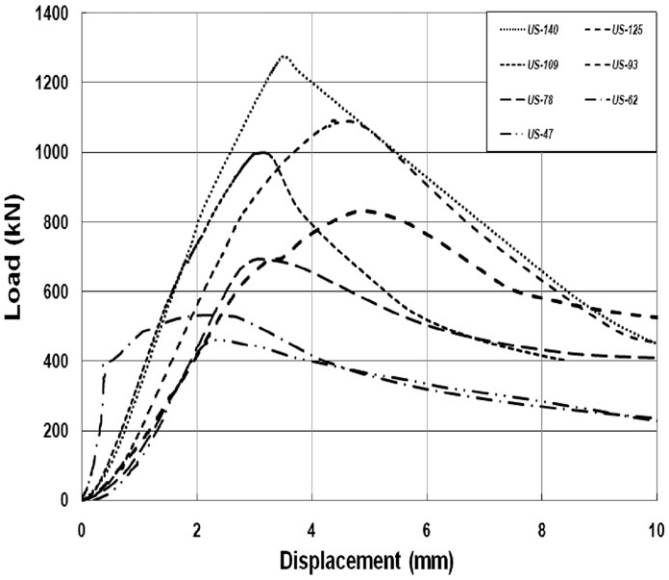

Fig. 3. Axial load versus shortening curves of CHS sections.

Table 3
Local buckling and maximum stresses of CHS columns.

Sections	D/t	f_{max}(MPa)		f_{crl}(MPa)	
		Nonlinear analysis	Tests	Tests	Elastic analysis
US-47	47	265	306	272	3177
US-62	62	261	265	243	2362
US-78	78	259	273	229	1952
US-94	93	258	273	200	1746
US-109	109	258	281	200	1619
US-125	125	257	267	208	1540
US-140	140	256	278	185	1495

Fig. 2. Failure modes of CHS columns.

specifications (2005) [4], AASHTO specifications (2007) [5] and Eurocode3 (2003) [9] seems to be slightly conservative in consideration of the test results.

3.2. Circular concrete-filled tubular (CFT) column tests

A series of compression tests were performed in the same method as for CHS columns. A concentric compression test was conducted using a 3000 kN or a 5000 kN Shimazu Universal Testing Machine to account for the size of CFT columns. The test set-up with a 5000 kN testing machine is shown in Fig. 4. As the load was increased to the local buckling load, the steel skin of the circular CFT columns bulged outwardly at several locations along the columns. Local buckling in the so-called 'lantern buckling' mode was observed for all test sections. The general collapse modes of circular CFT columns are shown in Fig. 5. Because of the filled-in concrete, the collapse modes of circular CFT composite columns were quite different from those of CHS sections, which are shown in Fig. 2. Since the inward deformation of the steel skin was restrained by the filled-in concrete, the buckled shape was symmetrical and one or two bulges finally remained before the rupture of the welds at the location of maximum bulge along the column. Either the crack of filled-in concrete or the local buckling of the steel skin made the columns lose structural stiffness. It was impossible to decide which, the crack of the filled-in concrete or the local buckling of the steel skin, occurred first. However, the crack propagation of concrete did not cause the sharp drop of load until the final collapse of the sections because of the restraint of the steel skin. The confining effect of the steel skin of low D/t ratio against the filled-in concrete did not decrease significantly in spite of the local buckling.

Axial load versus shortening curves are shown in Fig. 6. After an initial take-up, the linear load versus shortening relationship was exhibited until the occurrence of local buckling of the steel skin or crack of the filled-in concrete. After local buckling, the axial load versus shortening curve became rounded, and the stiffness reduced. However, the load level was increased continuously up to the ultimate load. Contrary to the axial load versus shortening curves of CHS sections, which commonly displayed a sharp drop in loading after the maximum load was reached, those of the circular CFT sections did not show a decrease in loading until the final failure. All the circular CFT columns displayed a stable and ductile behavior until the rupture of the welds. Though a large deformation in a local buckling mode may significantly

Fig. 4. Test set-up (5000 kN testing machine).

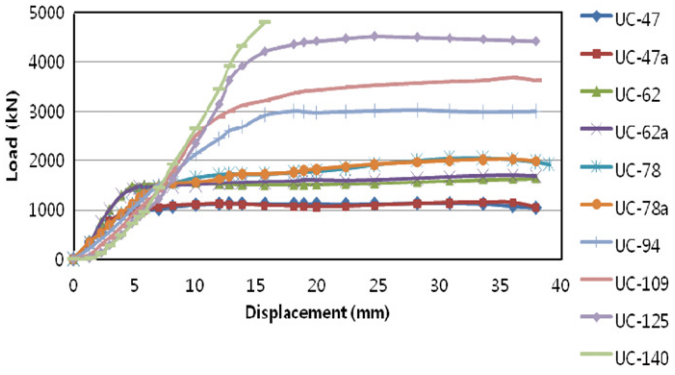

Fig. 6. Axial load versus shortening curves of circular CFT composite columns.

Fig. 5. Collapse modes of circular CFT columns.

Table 4
Ultimate and buckling loads of circular CFT columns.

Sections	Tests				P_u(kN) Eq. (1)	P_{max}/P_u
	P_{max}(kN)	f_{max}(MPa)	P_{cr}(kN)	f_{cr}(MPa)		
UC-47	1129	378.9	1020	342.7	811	1.39
UC-47a	1123	380.9	1000	339.2	802	1.40
UC-62	1535	327.9	1410	301.2	1261	1.22
UC-62a	1560	335.8	1450	312.1	1250	1.25
UC-78	2033	293.0	1720	247.9	1841	1.10
UC-78a	2012	290.0	1650	237.8	1841	1.09
UC-94	3000	317.1	2320	245.2	2510	1.20
UC-109	3680	296.3	2985	240.5	3279	1.12
UC-125	4540	286.8	3771	238.2	4166	1.09
UC-140	–	–	4484	230.0	5116	–

reduce the confining force of the steel skin and the outward deformation of filled-in concrete cannot be retained, the compressive stress of the cracked concrete may be maintained in the tri-axial loading stage. Since the UC-140 section was not failed at the load of 4700 kN, the increase of loading was terminated during testing for the safety of machine.

Even if the magnitude of the concrete compressive strength is slightly differently defined in the current specifications such as AISC (2005) [4], AASHTO LRFD (2007) [5] and Eurocode4 (2004) [3], the ultimate strength or the squash load of a concrete-filled composite stub column is generally given by

$$P_u = F_y A_s + K_c F_c A_c \tag{1}$$

where F_y=steel yield stress; A_s=steel area; F_c=concrete compressive strength; A_c=concrete area and the factor K_c is generally taken as 0.85, 0.95 or 1.0 according to the type of composite column and the shape of the cross section.

The test local buckling and the maximum loads of the test columns are summarized in Table 4, where P_{max} and P_{cr} indicate the maximum load and the local buckling load obtained by tests, respectively. Maximum and local buckling stresses were calculated based on the effective cross section area under an assumption that the steel-to-concrete elasticity ratio was 9.0. As shown in Table 4, both the confining effect of the filled-in concrete by the steel skin and the restraining effect against the inward deformation of the steel skin by the filled-in concrete increased the ultimate strength of the concrete-filled tubular composite sections significantly. However, the amount of strength enhancement due to the co-relational effect was different among the test sections, mainly due to the differences of the plastic strength ratio between the steel skin and the filled-in concrete. The maximum stresses of the circular CFT sections were much higher than the test yield stress of the material, which was much higher than the nominal yield stress of the material. The maximum and the local buckling stresses of the circular CFT sections were much higher than those of the CHS sections. The maximum load of the test sections measured was larger than the squash load computed by Eq. (1) with k taken as 1.0. The ratios of the test maximum load to the squash load obtained by Eq. (1) ranged 1.09–1.40 and showed a decreasing trend with the increase of the D/t ratio, except at section UC-94.

4. Ultimate strengths of concrete-filled tubular section columns

4.1. Direct strength curves for circular and rectangular hollow steel section columns

To account for the local buckling of CHS and RHS columns in the column strengths, the AISC specifications (2005) [4] provides the effective width formula (Q-factor). The Eurocode3 (2003) [9] also adopts the effective width method for RHS columns, but recommends reference to 'part 1–6: Design of Shell Structures' for CHS columns of category 4. The Direct Strength Method (DSM) offers a simple and designer-friendly approach to predicting the load capacity of steel sections. DSM strength equations for cold-formed steel sections undergoing local and overall buckling interaction were adopted by NAS Appendix 1(AISI, 2004) [6] and AS/NZS 4600(AS, 2005) [7] recently. Based on the welded H- and C-section column tests, a similar set of equations for welded sections were derived to account for the interaction between local and overall buckling [10].

$$P_{nl} = P_{ne} \quad \text{for } \lambda \le 0.816 \tag{2a}$$

$$P_{nl} = \left(1 - 0.15\left(\frac{P_{crl}}{P_{ne}}\right)^{0.5}\right)\left(\frac{P_{crl}}{P_{ne}}\right)^{0.5} P_{ne} \quad \text{for } \lambda > 0.816 \tag{2b}$$

in which

$$\lambda = \sqrt{P_{ne}/P_{crl}} \tag{2c}$$

In Eqs. (2a)–(2c), P_{nl}=limiting strength accounting for local and overall buckling (N); $P_{crl}=F_{crl}A$=elastic local buckling load (N); $P_{ne}=F_{ne}A$=overall column strength based on the overall failure mode (N), which is determined from the minimum of the elastic flexural, torsional and flexural–torsional buckling stresses. The overall column strength, F_{ne}, can be calculated from Eqs. (E3-2) and (E3-3) of the AISC [5] or Eqs. (6.47), (6.48) and (6.49) in the Eurocode 3 [9] or the equations in Table 3.3.2 of the KHBDS [11].

The test and FE analysis results [12] of the CHS sections failed in the local mode are compared with Eqs. (2a) and (2b), NAS DSM curve [6] and AISC Q-factor curve [4] in Fig. 7. Previous test results for RHS columns [13] are also included in Fig. 7 for comparison. The AISC Q-factor curves are converted as a function of λ and are shown in Fig. 7 for comparison. Referring to Fig. 7, it is clear that the NAS DSM curves [6] adopted in the cold-formed steel codes and Eqs. (2a) and (2b) proposed in the welded H- and C-sections are generally conservative for RHS sections, except for the sections with slenderness of around 0.9. Therefore, it seems reasonable to apply Eqs. (2a) and (2b) based on the H- and C-section column tests to RHS columns. However, at first glance, the NAS DSM [6] and Eqs. (2a), (2b) are non-conservative for CHS columns with local slenderness values of $0.5 < \lambda < 0.8$. On the contrary, the AISC Q-factor curves underestimate the section capacity for the CHS column tests. A similar set of strength equations has been derived for the CHS columns. A comparison of test results with the strength curves (3a) and (3b) is also shown in Fig. 7. The design curves take a similar form to those of the NAS

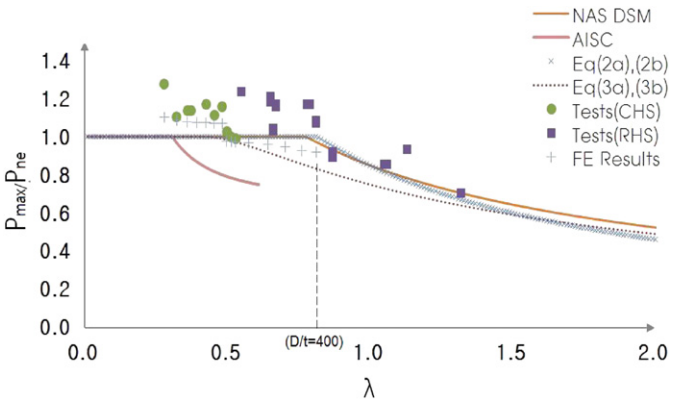

Fig. 7. Comparison of DSM curves and test results.

DSM but differ only with respect to the constant of 0.25, which is 0.15 in NAS DSM. The constant 0.25 reflects a slightly lower post-local-buckling strength reserve than that of open section columns. It is clear that Eqs. (3a) and (3b) can provide a safe envelope of strength for both CHS and RHS sections. Detailed evaluation of the proposed curves can be found in Kwon and Kang (2009) [12].

$$P_{nl} = P_{ne} \quad \text{for } \lambda \le 0.420 \tag{3a}$$

$$P_{nl} = \left(1.0 - 0.25\left(\frac{P_{crl}}{P_{ne}}\right)^{0.4}\right)\left(\frac{P_{crl}}{P_{ne}}\right)^{0.4} P_{ne} \quad \text{for } \lambda > 0.420 \tag{3b}$$

where

$$\lambda = \sqrt{P_{ne}/P_{crl}} \tag{3c}$$

4.2. Design strength of concrete filled tubular (CFT) sections

4.2.1. Current specifications

The column strength formula given in Eq. (1) is generally adopted for the resistance of CFT stub columns in the current specifications, where the factor k is taken as 0.85, 0.95 or 1.0 according to the type of composite column and the shape of the cross section. The strength formula can satisfactorily be used whenever the steel section yields first before local buckling takes place. In current specifications such as AISC (2005) [4], AASHTO (2007) [5] and Eurocode4 (2004) [3], to prevent local buckling in the steel skin of CFT composite columns, the width to thickness ratio and the exterior diameter to thickness ratio are limited. Even though the formulae for the maximum D/t ratio in other current specifications seem to be slightly different, the limitations range approximately from 80 to 100. However, in the AASHTO specifications (2007), higher ratios are permitted when their use is justified by test or analysis. However, clear provisions for these ratios accounting for the local buckling of the steel skin of CFT columns cannot be found in any current specification. Whenever the sections with ratios higher than the maximum limit are used, local buckling should be accounted for in the prediction of design strengths for CFT columns. One way to take local buckling into consideration is to adopt the effective width method for thin-walled steel sections. Since the local buckling mode and the effective width of the steel skin of CFT sections are quite different from those of hollow steel sections of same geometries, the effective width formula for CFT sections should be different from that for hollow steel sections. However, the effective width formula for the CFT sections cannot be found in any current specification, as far as the authors know. In a series of compression tests conducted in this research, even the sections satisfying the limitations of the diameter to thickness ratio, provided by the current design specifications, showed local buckling in the steel skin of the circular CFT sections during testing. Therefore, for the accurate prediction of the member strength of the circular CFT columns, a rational design method to account for the local buckling of the steel skin needs to be developed.

In the plastic resistance of stub columns to compression represented by Eq. (1) in AISC specifications (2005), the factor K_c is taken as 0.85 for rectangular CFT columns and 0.95 for circular CFT columns. In Eurocode4 [3], the factor K_c may be taken as 1.0 for concrete-filled composite sections. However, for circular sections, the increase in strength of concrete caused by confinement may be accounted for as

$$K_c = 1 + \eta_1 \frac{t}{D}\frac{F_y}{F_c} \tag{4}$$

where

$$\eta_1 = 4.9 - 1.85\lambda + 17\lambda^2 \tag{5}$$

in which

$$\lambda = \sqrt{P_u/P_{cr}} \tag{6}$$

$$P_{cr} = \frac{\pi^2 (EI)_e}{l^2} \tag{7}$$

$$(EI)_e = E_s I_s + 0.8 E_c I_c \tag{8}$$

However, when the concrete strength is increased, the strength of steel, F_y, is replaced by $0.25(3+2\lambda)F_y$ to account for the decrease in the effective stress. In Korean Building Code (2005) [14], the factor K_c is taken as

$$K_c = 0.85\left(1 + 1.8\frac{t}{D}\frac{F_y}{F_c}\right) \tag{9}$$

4.2.2. Proposed squash load for CFT stub columns

As explained briefly in the previous section, in the current specifications such as Eurocode4 (2003), AISC specifications (2005) and AASHTO specifications (2007), the nominal yield stress of steel is generally adopted for the design strength for the steel of composite columns, as shown in Eq. (1). For the concrete-encased composite sections and the concrete-filled composite sections of low D/t ratio for circular shapes and low b/t ratio for rectangular shapes, the current specifications can be reasonably used. However, since a thin steel skin of higher ratios is generally used for the circular and rectangular CFT sections, local buckling in the steel skin should be considered in the prediction of the ultimate strength. Up to now, the effective width method has been the only way to account for the local buckling of the steel skin. However, since the effective width of the section is dependent on the stress level, its calculation should be conducted repeatedly by the trial–error method. Moreover since the effective width formulae in current design specifications are generally the same as those for steel sections, the effective width of CFT sections may be too conservative. To overcome this problem, the squash load of CFT stub columns can be expressed by Eq. (10).

$$P_u = F_{sd} A_s + K_c F_c A_c \tag{10}$$

where F_{sd}=steel design strength; A_s=steel area; F_c=concrete compressive strength; A_c=concrete area. The portion of the reinforcement steel bar area is omitted in Eq. (10) for simplicity.

Substituting the test ultimate load, $P_{\max}$, for P_u in Eq. (10), the member strength of the steel skin, F_{sd}, generalized by the nominal yield stress can be given by

$$F_{sd}/F_y = \frac{P_{\max} - K_c F_c A_c}{F_y A_s} \tag{11}$$

Since the local buckling stress of steel skins is generally increased by filled-in concrete, the DSM design curves for CHS columns in Eqs. (3a) and (3b) can be adopted conservatively for the design strength curves for the steel skin of CFT columns. The design strength curves of a steel skin is expressed in terms of stress by

$$F_{sd}/F_y = 1.0 \quad \text{for } \lambda \le 0.420 \tag{12a}$$

$$F_{sd}/F_y = \frac{1.0}{\lambda^{0.8}} - \frac{0.25}{\lambda^{1.6}} \quad \text{for } 0.420 < \lambda \tag{12b}$$

where

$$\lambda = \sqrt{F_y/F_{crl}} \tag{12c}$$

The elastic local buckling stress, F_{crl}, can be computed by rigorous computer programs. The well known theoretical equation

given in Eq. (13a) can be used for circular sections without longitudinal stiffeners, and Eq. (13b) for square sections and rectangular sections of equal width sub-panels. Eq. (13a) can be reasonably used for circular CFT sections, since it is valid for short buckle wave-lengths in longitudinal directions.

$$F_{crl} = \frac{2E}{\sqrt{3(1-\nu^2)}}(t/D) \quad \text{for circular sections} \tag{13a}$$

$$F_{crl} = \frac{4\pi^2 E}{12(1-\nu^2)}(t/b)^2 \quad \text{for rectangular sections} \tag{13b}$$

The design curves are compared with various test results in Fig. 9(a) and (b), where the value K_c in Eq. (10) is assumed as 1.0 and 0.85, respectively. Referring to Fig. 9(a) and (b), the design curve with K_c of 1.0 is non-conservative for many CFT column test results in the range $\lambda > 0.70$ and that with 0.85 is too conservative for most test results of CFT columns.

The factor K_c is mainly dependent on the confining effect provided by the steel skin against filled-in concrete. The confining effect of the steel skin differs according to the steel contribution ratio and the local buckling resistance of the steel skin. To account for the confining effect provided by a steel skin, the factor K_c can be proposed as Eq. (14)

$$0.85 \le K_c = 0.85\left(1+0.045\sqrt{\delta}\frac{F_{sd}}{F_c}\right) \le 1.0 \tag{14}$$

where the steel contribution ratio

$$\delta = F_y A_s/(F_y A_s + F_c A_c) \tag{15}$$

Eq. (14) is compared with those in Korean Building Code (2005), AISC specifications (2005) and Eurocode 4 (2004) in Fig. 7. To draw the curves in Fig. 8, the strengths of steel and concrete were assumed as 240 and 24 MPa, respectively, Poisson's ratio 0.3 and Young's modulus 205,000 Mpa. As shown in Fig. 8, the K_c obtained by KBC agreed well with Eurocode 4 with $\lambda = 0.2$. However, Eurocode 4 replaces the strength of steel, F_y, with $0.25(3+2\lambda)F_y$ to account for the decrease in the effective stress of the steel skin, but KBC uses the F_y without considering it. The value of K_c is taken as 0.95 in AISC (2005) for circular sections. Eq. (14) can provide reasonable values of K_c accounting for the increase of concrete strength, due to confinement of the steel skin. K_c is expected to lie between that of KBC and that of Eurocode4 ($\lambda = 0.1$) in the range of D/t from 100 to 400. When D/t is smaller than 100, in KBC and Eurocode4, K_c is larger than 0.85. For short columns, the concrete strength is increased over $1.0F_c$ due to the confinement of the steel skin. However, in Eq. (14), $1.0F_c$ was used as the cut-off line for the concrete strength to account for the micro-cracking in the concrete and to predict a conservative strength.

The steel design strengths F_{sd} predicted by Eqs. (12a) and (12b) are compared with test results expressed by Eq. (11) in Fig. 9(c), where the factor K_c was given by Eq. (14). The previous test results (Han [15]; Song and Kwon [16]; Kim and Jeon [17]; O'shea and Bridge [18]; Uy [19,20]; Ge and Usami [21]; Lee and Kwon [22]) are also included in Fig. 9(a)–(c) for comparison. As shown in Fig. 9(c), Eq. (14) for K_c is quite reasonable except in comparison to Ge and Usami's test results [20]. Test results have shown that circular CFT sections display more enhancements in an ultimate

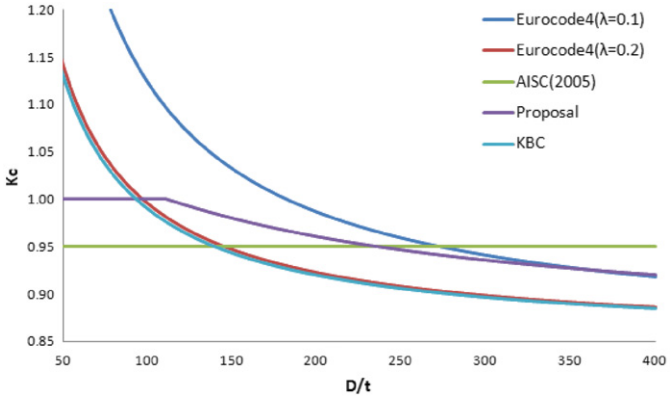

Fig. 8. Comparison of factor K_c between specifications for CFT columns: (a) $K_c = 1.0$, (b) $K_c = 0.85$ and (c) $K_c =$ Eq. (14).

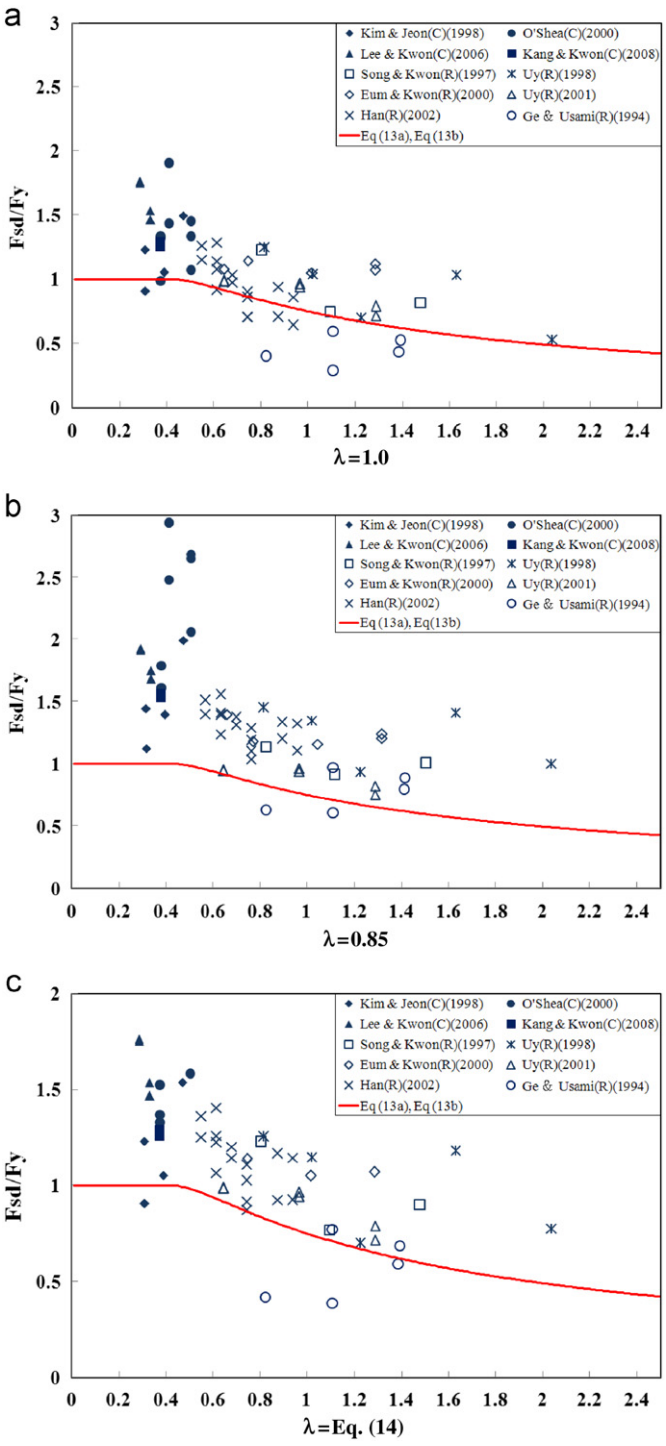

Fig. 9. Comparison of design strengths and test results for steel skin.

strength than rectangular ones. Therefore, the design strengths of the steel skins, of circular CFT sections, obtained by Eqs. (12a) and (12b) were more conservative than those of the rectangular CFT sections in comparison with the test results, as shown in Fig. 9(c). It can be concluded that the design strengths of the steel skin for the CFT columns obtained with Eqs. (12a) and (12b) rather than those predicted with fixed values of 0.85 or 1.0, agreed better with the test results.

4.2.3. Proposed resistance of CFT columns

The nominal compressive resistance of circular and rectangular CFT columns can be proposed by simple modification of the steel column strength formulae in the Korean Highway Bridge Design Specifications (2005) [11]. The design strength formulae for CFT columns can be proposed in terms of strength as

$$P_n = P_u \quad (\lambda_c \le 0.2) \tag{16a}$$

$$P_n = (1-0.419\lambda_c)P_u \quad (0.2 < \lambda_c \le 1.0) \tag{16b}$$

$$P_n = \frac{P_u}{0.773+\lambda_c^2} \quad (1.0 < \lambda_c) \tag{16c}$$

where P_u=ultimate strength given by Eq. (10)

$$\lambda_c = \sqrt{P_u/P_{cr}} \tag{17}$$

$$P_{cr} = \frac{\pi^2 (EI)_e}{l^2} \tag{18}$$

$$(EI)_e = E_s I_s + 0.8 E_c I_c \tag{19}$$

The effective flexural stiffness $(EI)_e$ in Eq. (19) is adopted from the Eurocode4 (2004).

The design strengths of the CFT columns predicted by the strength formulae proposed are compared with the strengths computed according to the AASHTO specifications (2007) and Eurocode4 (2004) in Table 5. As shown in Table 5, all the predicted design strengths for the CFT sections by AASHTO specifications, Eurocode4 and the proposed strength formulae are very conservative compared to most of all the test results, except for some test results of Kim and Jeon [17] and Ge and Usami [21]. As shown in Table 5(a), since the local buckling slenderness $\lambda = \sqrt{F_y/F_{crl}}$ for the circular CFT sections tested by the researchers ([12,16,17,18]) is generally less than 0.42, there is little difference in the design strengths predicted by the specifications. However, as shown in Table 5(b), in the case of the rectangular CFT sections such uc-12, uc-15, u9-c, u12-c, u12-hc, s75-c(1), s75-c(0.35) of comparatively larger local buckling slenderness, the Eurocode4 (2003) and the AASHTO specifications (2007) predicted the resistances of the composite sections non-conservatively in comparison with the test results. It is due to the higher width to thickness ratio than the limitation in those specifications. These sections of higher width to thickness ratios underwent local buckling before yielding of the steel skin. However, the column strengths predicted by the proposed strength formulae are nearly conservative in comparison with test results, except u9-c and u12-c. Consequently, it can be concluded that the design strengths predicted by the proposed strength formulae are conservatively acceptable without limitations for width to thickness ratio or diameter to thickness ratio, when compared with the test results and current specifications.

Table 5
Comparison of ultimate strengths of CCFT and RCFT columns (unit: kN).

Researcher	Specimens	Tests	EC4	AASHTO	AISC	Proposal
(a) CCFT						
Kim and Jeon (1998)	SC-CF45	5374	4992	4983	5302	5474
	SC-CF45a	9810	8157	8141	8662	8941
	SC-CF70	4867	4286	4277	4607	4784
	SC-CF101	8159	8792	8752	9311	9518
O'Shea (2000)	s30cs50b	1662	1342	1339	1434	1487
	s20cs50a	1678	1242	1239	1350	1364
	s16cs50b	1695	1404	1400	1531	1530
	s30cs80a	2295	1883	1877	2035	2021
	s20cs80b	2592	2021	2015	2215	2116
	s16cs80a	2602	2147	2139	2355	2248
	s30cs10a	2673	2354	2345	2557	2477
	s20cs10a	3360	2791	2780	3068	2872
	s16cs10a	3260	2796	2783	3073	2883
Lee and Kwon (2006)	UC-47	1129	748	746	788	811
	UC-47a	1123	740	739	780	802
	UC-62	1535	1150	1147	1220	1261
	UC-62a	1560	1141	1138	1210	1251
Kang and Kwon (2008)	UC-78	2012	1663	1659	1776	1841
	UC-78a	2034	1663	1659	1776	1841
(b) RCFT						
Ge and Usami (1994)	u9-c	1842	2207	2236	2204	2239
	u12-c	3067	3579	3475	3575	3479
	u12-hc	3998	4030	3908	4024	3913
	s75-c(1)	5027	5392	5065	5378	5078
	s75-c(0.35)	5155	5338	5029	5325	5040
Song and Kwon (1997)	uc9	1161	963	962	962	949
	uc12	1627	1636	1634	1633	1588
	uc15	2411	2309	2305	2305	2157
	LB1	1133	933	932	932	944
	LB3	1700	1507	1505	1505	1476
Uy (1998)	LB5	1500	1539	1538	1538	1478
	LB7	3095	2733	2730	2729	2549
	LB9	4000	3994	3989	3989	3680
Eum and Kwon (2000)	uc9	749	647	646	646	649
	uc12	1140	1021	1020	1020	991
	uc15	1665	1472	1470	1470	1409
	sc(2)15	1787	1553	1551	1551	1459
	sc(4)15	1935	1716	1714	1714	1793
Uy (2001)	hss 1	1836	1813	1809	1809	1855
	hss 2	1832	1813	1809	1809	1855
	hss 8	2868	2900	2894	2894	2451
	hss 9	2922	2900	2894	2894	2451
	hss 14	3710	4163	4155	4155	3278
	hss 15	3483	4163	4155	4155	3278
Han (2002)	rc 1-1	759	701	701	700	725
	rc 1-2	799	701	701	700	725
	rc 2-1	991	964	964	962	975
	rc 2-2	1049	964	964	962	975
	rc 3-1	843	762	762	760	778
	rc 3-2	859	762	762	760	778
	rc 4-1	1419	1304	1304	1301	1285
	rc 4-2	1339	1304	1304	1301	1285
	rc 5-1	554	474	474	473	504
	rc 5-2	576	474	474	473	504
	rc 6-1	640	550	550	548	567
	rc 6-2	672	550	550	548	567
	rc 7-1	799	752	752	749	757
	rc 7-2	759	752	752	749	757
	rc 8-1	1043	984	984	981	972
	rc 8-2	1085	984	984	981	972

5. Conclusions

A series of compression tests of circular hollow sections (CHS) and circular concrete-filled tubular (CFT) sections were conducted to investigate the correlation between filled-in concrete and steel skin, and the squash load of CFT composite stub columns.

The circular CFT columns showed a significant enhancement in the local buckling strength in comparison with the CHS columns. A squash load formula was proposed based on the CFT column test results conducted and previous test results of many

researchers. To estimate the ultimate strength of the steel skin of CFT stub columns which undergo local buckling, a simple strength formula for Direct Strength Method was adopted. The design strength of filled-in concrete was also proposed to account for the confinement effect, due to the strength ratio between steel skin and filled-in concrete, and the local buckling stress of the steel skin. The squash load formula proposed can predict the ultimate strength of CFT stub columns conservatively. The ultimate strengths of CFT columns predicted by AASHTO specifications (2007), Eurocode4 (2004) and the proposed strength equations were in good agreement with the test results of the CFT columns of comparatively low diameter to thickness (D/t) and width to thickness (b/t) ratios, respectively. However, in the case of rectangular CFT columns of higher width to thickness ratio than the limitation in the current specifications, the current specifications showed non-conservative strengths for the rectangular CFT columns in comparison with the test results. The ultimate strength predicted by procedures proposed showed good agreement with tests results of CFT columns, with either low or high width to thickness ratios. Therefore, it can be concluded that the proposed squash load formula can predict the ultimate strength for the CFT columns reasonably. However, the strength formulae should be calibrated further against various test results for the CFT columns of comparatively large diameter to thickness ratios for practical use.

Acknowledgement

This work was supported by the 2008 research grants from the Yeungnam University.

References

[1] Chen WF, Atsuta t. Theory of beam-columnA—volume 1: in-plane behavior and design. New York: McGraw-Hill; 1991.
[2] Bradford MA. Design of short concrete-filled RHS sections. Civil Engineering Transactions, Institution of Engineers, Australia 1991;CE33(3):189–94.
[3] European Committee for Standardisation (ECS). Eurocode 4: design of composite steel and concrete structures, Part 1-1: general rules and rules for buildings. Brussels, Belgium; 2004.
[4] American Iron and Steel Construction (AISC). Specification for steel structural buildings. Chicago, IL, USA; 2005.
[5] American Association of State Highway and Transportation Officials (AASHTO). AASHTO LRFD bridge design specifications. Washington D.C.; 2007.
[6] American Iron and Steel Institute.North American specifications for the design of cold-formed steel structural members, Supplement no. 1. Washington DC, USA; 2004.
[7] Standards Australia. Cold-formed steel structures AS/NZS 4600: 2005. Sydney, NSW, Australia;. 2005.
[8] FEA Co., Ltd.. Lusas element reference manual & user's manual (version 14.3); 2009.
[9] European Committee for Standardisation (ECS). Eurocode 3: design of steel structures, Part 1-1: general rules and rules for buildings. Brussels, Belgium; 2003.
[10] Kwon YB, Kim NK, Hancock GJ. Compression tests of welded section columns undergoing buckling interaction. Journal of Constructional Steel Research 2007;63:1590–602.
[11] Korean Association of Highway and Transportation Officials. Korea highway bridge design specifications. Seoul, Korea; 2005.
[12] Kang DW, Kwon YB. A study on the structural behavior and strength of circular hollow section columns. Journal of Korean Society of Steel Construction 2009;21(5):505–14. in Korean.
[13] Um CS, Song JY, Kwon YB. An experimental study on the structural behavior of welded steel box piers. Journal of Structural Engineering, KSCE 2001;2(6-A):837–848. in Korean.
[14] Korean Association of Building and House Officials. Korean building codes. Seoul, Korea; 2005.
[15] Han LH. Tests on stub columns of concrete-filled RHS sections. Journal of Constructional Steel Research 2002;58(3):353–72.
[16] Song JY, Kwon YB. An experimental study on the ultimate strength of concrete-filled rectangular stub columns. Journal of Korean Society of Civil Engineering 1997;17(1–4):607–15. in Korean.
[17] Kim JH, Jeon SH. An experimental study on the ultimate strength of concrete-filled stub columns. Journal of Steel Structures (in Korean), Korean Society of Steel Construction 1999;11(5):495–506.
[18] O'Shea MD, Bridge RQ. Design of circular thin-walled concrete-filled steel tubes. Journal of Structural Engineering 2000;126(10–12):1295–303.
[19] Uy B. Local and post-local-buckling of concrete filled steel welded box columns. Journal of Constructional Steel Research 1998;47(1–2):47–72.
[20] Uy B. Strength of short concrete filled high strength steel box columns. Journal of Constructional Steel Research 2001;57(2):113–34.
[21] Ge HUsami T. Development of earthquake-resistant ultimate strength design method for concrete filled steel structures. Research Report no. 1994-1, Nagoya University, Japan; 1994.
[22] Lee JHKwon YB. The ultimate strength of concrete-filled steel composite columns. In: Proceedings, IABSE2007, Weimar; 2007, p. 500–1.